

Study of Nb₃Sn Strands for Fermilab's High Field Dipole Models

Emanuela Barzi, Peter J. Limon, Ryuji Yamada, and Alexander V. Zlobin

Abstract—Fermilab is developing 11 T superconducting dipole magnets for future accelerators based on Nb₃Sn conductor. Multifilamentary Nb₃Sn strands 1 mm in diameter produced with the Modified Jelly Roll and Powder-in-Tube technologies were purchased from OST and SMI respectively. They are herein fully characterized by I_c, n-value, residual resistivity ratio, and magnetization. Results of heat treatment optimization studies are also presented for the OST strand.

Index Terms—Critical current, magnetization, Nb₃Sn strand, superconducting magnet.

I. INTRODUCTION

WITHIN the framework of an R&D program towards a post-LHC Very Large Hadron Collider (VLHC), high field Nb₃Sn dipole magnets (HFM) with a field above 10 T are being developed at Fermilab. The first models feature 1 meter long two-layer shell-type (cos-theta) coils that use a keystone Rutherford-type cable made of 28 Nb₃Sn strands 1mm in diameter [1]. In such a design, the critical current density in the non-Cu section of the strand, J_c, that is needed at 4.2 K and 12 T to reach a maximum field of 11 T is in the 1800 to 2000 A/mm² range depending on the Cu to non-Cu ratio. Multifilamentary Nb₃Sn is one of the commercially available materials that can achieve this goal. About 11 km and 5.5 km of strands produced using the Modified Jelly Roll (MJR) and Powder-in-Tube (PIT) technologies were purchased by Fermilab from Oxford Superconducting Technology (OST) and ShapeMetal Innovation (SMI) respectively. In this paper, these round Nb₃Sn strands are characterized by I_c, n-value, residual resistivity ratio (RRR), and magnetization. Heat treatment (HT) studies are also presented for the OST strand.

II. EXPERIMENT

A. Strand Specifications

Fermilab's technical specifications for the OST and SMI strands are summarized in Table I. They were dictated by the magnet design and the specific features of each technology. The OST strand was produced out of three billets (ID 113, 114, and 115) with the MJR technology and 54 sub-elements. The SMI strand was produced out of four billets (ID 31, 34A, 34B, and 34C) with the PIT technology and 192 filaments and ternary (NbTa)₃Sn. Cross sections of the unreacted strands are shown in Figs. 1 and 2. Piece lengths and Cu fractions are given in Tables II and III.

Manuscript received September 17, 2000. The authors are with Fermilab, Batavia, IL 60510 USA (telephone: 630-840-3446, e-mail: barzi@fnal.gov).

This work was supported by the US Department of Energy.

TABLE I
STRAND SPECIFICATIONS

Parameter	OST Strand	SMI Strand
Strand diameter, mm	1.000±0.005	1.000±0.005
J _c (12 T, 4.2 K), A/mm ²	> 2000	> 1700
I _c (12 T, 4.2 K), A	> 785	> 800
d _{eff} , μm	< 105	< 50
Cu, %	45 ± 5	45 ± 5
RRR	> 75	> 100
Twist pitch, mm/turn	25 ± 10	20 ± 3

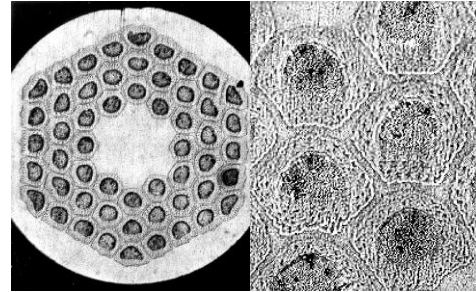


Fig. 1. Left: optical microscopy of an unreacted 1 mm OST strand. Right: zoom in the sub-elements (Courtesy Kelly Molnar, LBNL).

TABLE II
PIECE LENGTHS AND CU FRACTIONS OF OST STRAND

Billet ID	113	113	113	113	114	115	115
Spool No.	A1	A2	B1	B2	-	B	C
Length, m	687	1800	932	786	5554	490	540
Cu, %	48	47.5	47.6	48.2	48	48.1	48.2

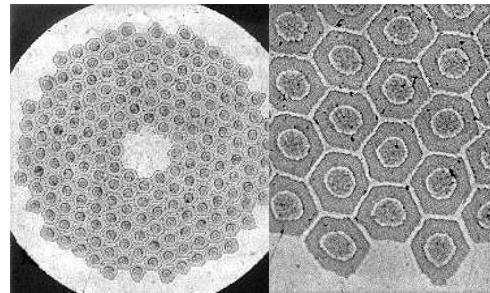


Fig. 2. Left: optical microscopy of an unreacted 1 mm SMI strand. Right: zoom in the filaments (Courtesy Kelly Molnar, LBNL).

TABLE III
PIECE LENGTHS AND CU FRACTIONS OF SMI STRAND

Billet ID	34A	34A	34A	34B	34B
Spool No.	AA	AB	BBA	AB	BB
Length, m	639	302	594	610	876
Cu, %	45.7	45.7	45.7	45.1	45.1
Billet ID	34C	34C	34C	31	
Spool No.	AA	AB	B	-	
Length, m	200	881	652	772	
Cu, %	45.3	45.3	45.3	45	

B. Strand Heat Treatments

To characterize the OST and SMI strands, several sets of samples were prepared and tested. The thermal cycles recommended by the companies are detailed in Table IV. The OST HT was applied to a set of five spools. The SMI HT was applied to back end samples of all spools. The originally recommended HT of 62 h at 675°C was applied to four front end samples (one per billet) with a ramp rate of 150°C/h.

A number of HT studies were carried out on a subset of OST spools according to the schedules given in Table V. In HT-8, the samples were let cool down to room temperature after the first step, and then re-heated with a ramp rate of 150°C/h directly up to 700°C. HT-1 to HT-7 were continuous from start to end, without any interruption. As a result of these studies, HT-3 (named *FNAL-HT* in the following) was adopted for the first dipole model. It was also applied to the complete set of OST spools.

TABLE IV
OST AND SMI HEAT TREATMENT CYCLES

Heat Treatment	Step 1	Step 2	Step 3	
OST	Ramp rate, °C/h	25	50	75
	Temperature, °C	210	340	650
	Duration, h	100	48	180
SMI	Ramp rate, °C/h	150	120	
	Temperature, °C	590	675	
	Duration, h	1/3	62	

TABLE V
HEAT TREATMENT STUDIES ON OST STRAND

Heat Treatment ^a	Step 1	Step 2	Step 3	
HT-1	Temperature, °C	575		
	Duration, h	200		
HT-2	Temperature, °C	575	700	
	Duration, h	200	30	
HT-3	Temperature, °C	575	700	
	Duration, h	200	40	
HT-4	Temperature, °C	575	700	
	Duration, h	200	50	
HT-5	Temperature, °C	575	700	
	Duration, h	200	60	
HT-6	Temperature, °C	600	700	
	Duration, h	200	60	
HT-7	Temperature, °C	210	575	700
	Duration, h	100	200	30
HT-8	Temperature, °C	575	Cool down	700
	Duration, h	200	to T _{room}	40

^a The temperature ramp rate is 25°C/h for all steps, but step 3 in HT-8 where it was 150°C/h.

C. Sample Preparation and Measurement Procedure

The samples used for I_c measurements were wound on grooved cylindrical Ti-alloy (Ti-6Al-4V) barrels, and held in place by two removable end rings [2]. Those for magnetization measurements were wound on stainless steel tubes. All sets were heat treated in argon atmosphere. After HT, the Ti-alloy end rings were replaced by Cu rings, and voltage-current (VI) characteristics were measured in boiling He at 4.2 K, in a transverse magnetic field from 12 T to 15 T. The voltage was measured along the sample by means of voltage taps placed 50 cm apart. The I_c was determined from the VI curve using the $10^{-14} \Omega \cdot m$ resistivity criterion. The relative directions of external magnetic field and transport

current were such as to generate an inward Lorentz force. Due to the latter and to the differential thermal contraction between sample and barrel, the specimen is subject to a tensile strain of up to 0.05 % at 12 T and 4.2 K. This leads to a systematic error in the 3 to 5 % range on I_c [3]. The n -values were determined in the $V(I_c)$ to $10 \cdot V(I_c)$ range by fitting the VI curve with the power law $V \sim I^n$. The estimated uncertainty of the I_c measurements is within ± 1 % at 4.2K and 12 T, and it is about ± 5 % for the n -values.

Magnetization measurements were performed using a balanced coil magnetometer. The uncertainty on magnetization is ± 1 % at 1 T, less than ± 4 % at 12 T, and within ± 6 % on the effective filament diameter, d_{eff} . [4].

III. RESULTS AND DISCUSSION

A. Critical Current, n -value, and RRR

In Fig. 3 are shown the I_c distributions for the SMI (*back* and *front* ends) and OST strands (*FNAL-HT*) at 12 T. The average I_c and the rms are also shown for each set. Fig. 4 shows the RRR distributions. The J_c 's and n -values averaged over all samples of each set are shown in Figs. 5 and 6 as a function of magnetic field.

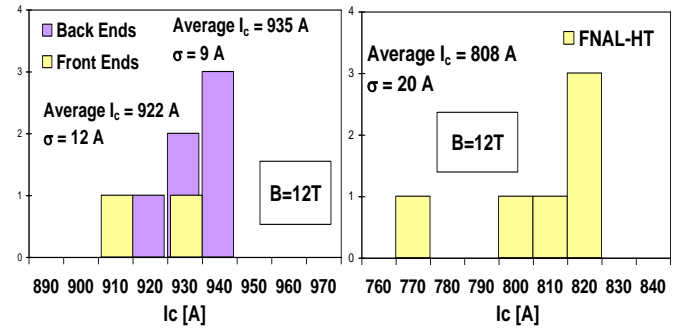


Fig. 3. I_c distribution of the SMI (left) and OST (right) strand at 12 T.

Both SMI and OST strands meet the I_c specs and are homogeneous in I_c . At 12 T it was uniform within ± 1 % for the SMI strand and within ± 2.5 % for the OST strand. The n -values are also high and quite uniform. At 12 T they were 58 ± 5 % for the SMI strand and 48 ± 7 % for the OST strand. The strand diameter was $1.005 \pm 0.002 \mu m$ for SMI and $1.002 \pm 0.002 \mu m$ for OST. The SMI strand also meets the RRR requirement, whereas the RRR of the OST strand is rather low. It is apparent that the Nb barriers leak Sn into the surrounding Cu stabilizer.

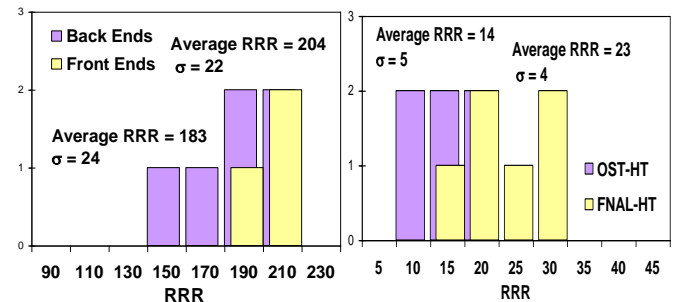


Fig. 4. RRR distributions for the SMI (left) and for the OST sets (right).

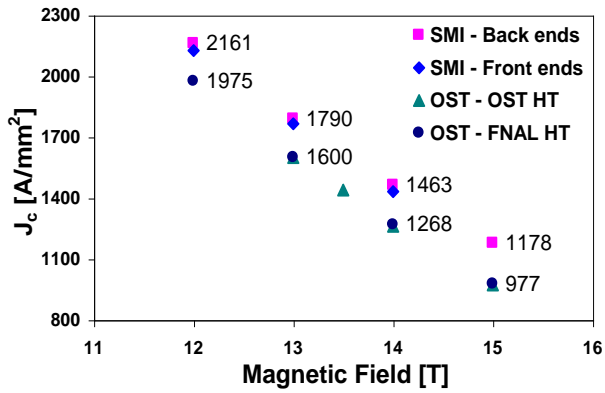


Fig. 5. Average J_c vs. magnetic field. The values are shown for the SMI back end set and for the OST set with FNAL-HT.

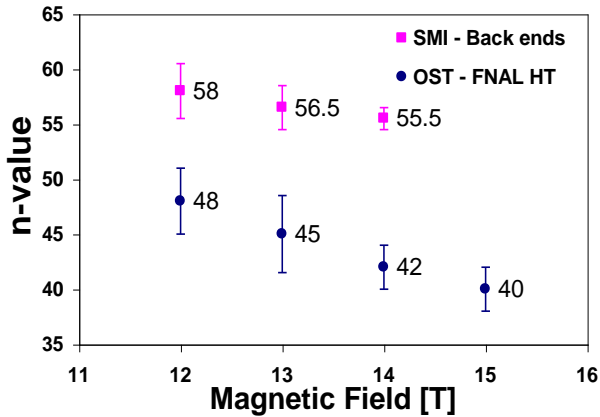


Fig. 6. Average n -value vs. magnetic field for the SMI back end set and for the OST set with FNAL-HT. Error bars represent the rms at a given field.

B. Magnetization and d_{eff}

In Fig. 7 are shown the magnetization curves (per non-Cu volume) performed with a field ramp rate of 17 mT/s between 0 and 3 T for an SMI strand and an OST strand with OST-HT. Several loops were completed to check reproducibility. Magnetic instabilities (flux jumps) are evident at low field in both shielding and trapping branches.

The d_{eff} was calculated directly from 13-10-13 T loops as shown in Fig. 8 by measuring $\mu_0\Delta M(12\text{ T})$ per total strand volume and $I_c(12\text{ T})$. The $\mu_0\Delta M(12\text{ T})$ was $32.8\pm 1.3\text{ mT}$ for SMI 34B-BB, and $62.8\pm 2.5\text{ mT}$ for OST 113A1. The calculated d_{eff} were $53\pm 3\text{ }\mu\text{m}$ and $115\pm 8\text{ }\mu\text{m}$ respectively. Both these values are very close to the specs.

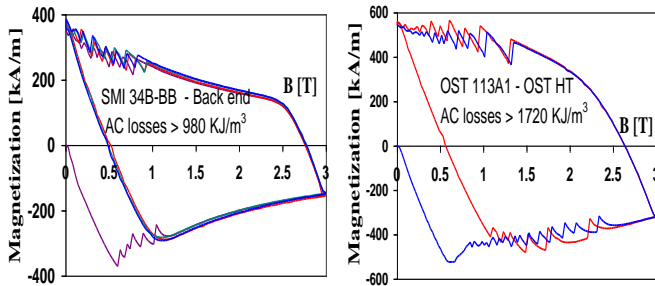


Fig. 7. Magnetization curves per non-Cu volume for an SMI strand (left) and for an OST strand (right). Non-Cu losses are given for 3-0-3 T loops.

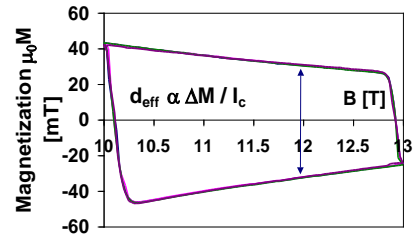


Fig. 8. Magnetization curve per total volume of an OST strand at high field.

C. Results of HT Optimization Studies

The effects of HT on J_c , n -value and RRR are shown in Figs. 9, 10, and 11 for OST strands 113B1 and 113B2. In these and in the following plots, data points with 0 h at 700°C are associated to HT-1 (*i.e.* only a step of 200 h at 575°C).

As shown in Fig. 9, HT's with a final step of higher temperature (*i.e.* 700°C) are 3 to 4 days shorter with respect to OST-HT and yield about the same J_c . They also provide higher n -values (see Fig. 10). It was found that the interruption of a HT after the first step at 575°C (*i.e.* HT-8) caused a 5 to 6 % I_c degradation. Power outages that occurred in the 575°C step lead to a 2 to 3 % I_c degradation. Such reductions in current are accompanied by proportional reductions in n -value.

Notice from Fig. 11 how the RRR is still high (100) at 575°C . Also, adding a low temperature (210°C) step does not improve the RRR, since HT-7 and HT-2 that differ only in this step produce a same RRR value of about 60. The low OST RRR values can be raised up to the 40 to 60 range by either keeping the HT time at 700°C below 30 h or interrupting the HT after the first step at 575°C .

Fig. 12 shows the low field magnetization curves for an OST strand with HT-6 and FNAL-HT. Flux jumps are substantially reduced with respect to Fig. 7 (right). In the case of FNAL-HT, they have totally disappeared from the shielding branch of second and further loops.

The effect of HT on d_{eff} is shown in Fig. 13. These results show, together with Fig. 14 (left), that after 200 h at 575°C (*i.e.* HT-1), the Nb_3Sn has already reached a considerable fraction of its full growth range.

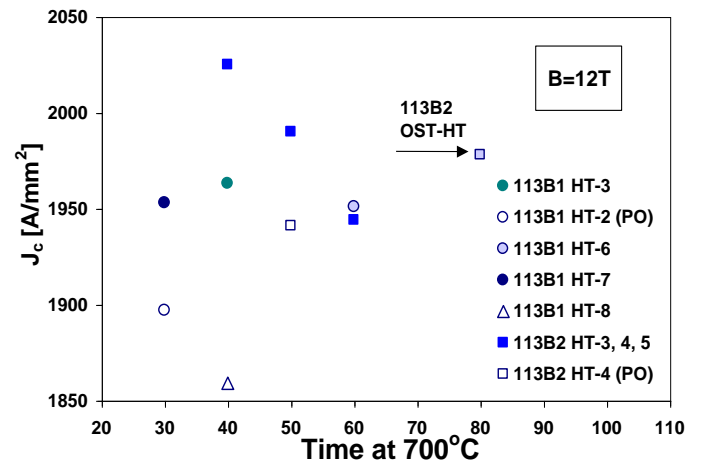


Fig. 9. J_c at 12T of two OST strands vs. HT time at 700°C . *PO* stands for power outage. The extrapolated J_c of 113B2 with OST-HT is also shown.

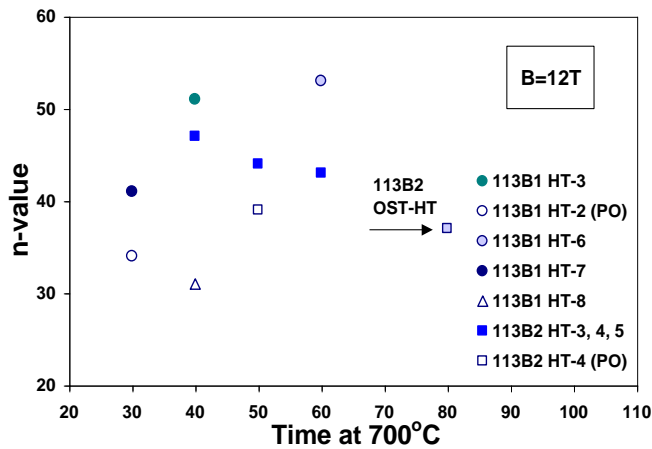


Fig. 10. n-value at 12T of OST strands vs. HT time at 700°C. PO stands for power outage. The extrapolated n-value of 113B2 with OST-HT is shown.

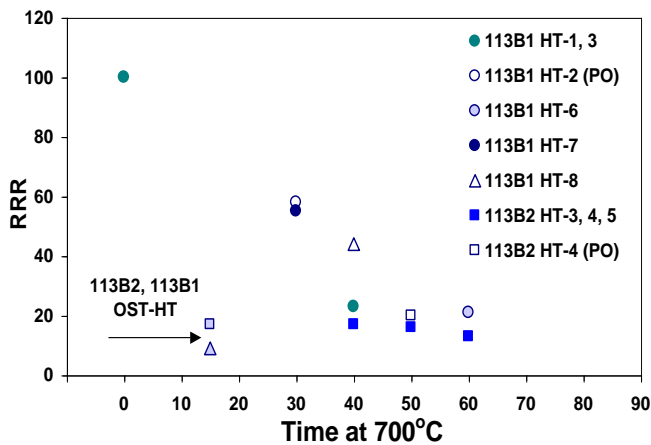


Fig. 11. RRR of two OST strands vs. HT time at 700°C. PO stands for power outage. The RRR of 113B1 and 113B2 with OST-HT are also shown.

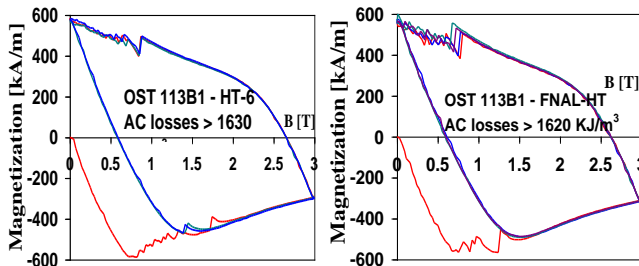


Fig. 12. Magnetization curves per non-Cu volume for OST strand 113B1 with HT-6 (left) and FNAL-HT (right).

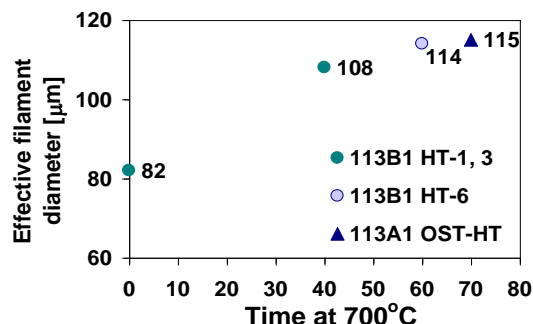


Fig. 13. d_{eff} of OST strand 113B1 vs. HT time at 700°C. The d_{eff} of strand 113A1 with OST-HT is also shown for comparison.

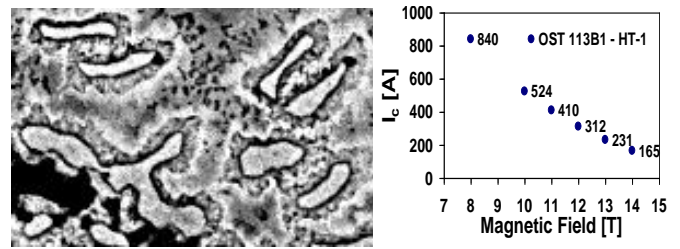


Fig. 14. SEM of partially reacted NbSn filaments (left) and I_c vs. magnetic field (right) for OST strand 113B1 with HT-1.

Fig. 14 (right) shows I_c as a function of field of an OST strand after HT-1. These data were fitted using [5] to infer B_{c20} , the upper critical field at $T=0$ K, and T_{c0} , the critical temperature at $B=0$ T. For HT-1, the best fits gave a B_{c20} of 21.5 ± 0.5 T and a T_{c0} of 17 ± 2 K. The same formulae were used to fit data from the other HT's, which all included a 700°C step. In such cases, the best fits gave a higher B_{c20} of 25.5 ± 0.5 T and a T_{c0} of 17 ± 2 K. As a comparison, fits performed on the SMI strand gave a B_{c20} of 27 ± 0.5 T and a T_{c0} of 19 ± 1 K.

IV. SUMMARY AND CONCLUSIONS

MJR and PIT Nb₃Sn strands produced by OST and SMI were fully characterized. The specs were met in all cases but the RRR for OST. It is apparent that for this strand the Nb barriers are too thin and not optimized to withstand for a long time even temperatures as low as 650°C. Hence, Sn diffusion contaminates the Cu stabilizer outside the barriers.

HT's with a short 700°C step proved to be advantageous in terms of time, n-value, and RRR. They also limited magnetic instabilities.

The I_c of a strand is reduced during magnet fabrication, due both to cabling and to cable compression in the coil. The former effect was addressed by systematic studies of I_c cabling degradation using Rutherford cables [8].

It should be noted that for future safe and reliable magnets with an operating margin of 15 % and a Cu to non-Cu ratio as high as 1.2, the J_c requirement at 12 T and 4.2 K is of 3000 A/mm². Also, the excellent field uniformity needed by accelerator magnets requires a d_{eff} of less than 30-40 μm [7].

REFERENCES

- [1] G. Ambrosio et al., "Development of the 11T Nb₃Sn dipole model at Fermilab", PAC'99, MT-16, Ponte Vedra Beach, FL, 1999.
- [2] L. F. Goodrich et al., "Superconductor critical current standards for fusion applications", NISTIR 5027, NIST.
- [3] E. Barzi et al., "Error analysis of short sample J_c measurements at the Short Sample Test Facility", FNAL TD-98-055¹, Sept. 1998.
- [4] C. Boffo, "Magnetization measurements at 4.2K of multifilamentary superconducting strands", FNAL TD-99-074¹, Dec. 1999.
- [5] J. McDonald and E. Barzi, "A model for J_c in granular A-15 superconductors", this Conference Proceedings.
- [6] E. Barzi et al., "Heat treatment optimization of internal tin Nb₃Sn strands", this Conference Proceedings.
- [7] G. Ambrosio et al., "Superconductor requirements for the HFM program at Fermilab", FNAL TD-99-073¹, Dec. '99.
- [8] E. Barzi et al., "Strand critical current degradation in Nb₃Sn Rutherford cables", this Conference Proceedings.

¹ Accessible from the web: <http://tdserver1.fnal.gov/tlibrary/TD-Notes/>.